PCCP

PAPER

View Article Online
View Journal | View Issue

Cite this: *Phys. Chem. Chem. Phys.*, 2025, **27**, 6794

Radical site-dependent exchange interactions in acridane-based bisnitroxides†

Yuta Takenouchi, Takuya Kanetomo * and Masaya Enomoto *

Received 18th November 2024,
Accepted 3rd March 2025

DOI: 10.1039/d4cp04393f

rsc.li/pccp

To investigate the radical site-dependence of exchange coupling in bisnitroxides, we have synthesized novel three acridane-based diradicals, *tert*-butyl nitroxide groups at the 2,7-, 2,6- and 3,6-positions of 10-benzyl-10′-methyl-9,9′(10*H*,10′*H*)spirobiacridine (**1-pp**, **1-mp** and **1-mm**, respectively). Theoretical and experimental magnetic studies indicate that **1-pp** and **1-mm** exhibit a singlet ground state, while **1-mp** exhibits a triplet ground state. These spin states can be explained by the spin polarization mechanism. Quantitative analysis revealed a difference in the magnitude of the exchange coupling constants between **1-pp** and **1-mm** owing to their local spin structures corresponding to 1,4- and 1,3-phenylene diradical motifs (Kekulé and non-Kekulé structures, respectively).

Introduction

Diradicals, which contain two unpaired electrons within a molecule, can exist in either a triplet (S = 1) or a singlet (S = 0) state due to intramolecular exchange coupling. These spin states depend on the molecular structure.[1] The triplet ground state requires orthogonality between the singly occupied molecular orbitals (SOMOs) to facilitate potential exchange interaction. This can be achieved by high molecular symmetry (*e.g.*, O_2 and spirodiradicals)[2,3] or by constructing a non-disjoint topological π-spin system (*e.g.*, trimethylenemethane).[4] Their high-spin configurations are promising building blocks for organic magnetic materials[5] and for metal complexes with paramagnetic ligands.[6] In contrast, the singlet ground state must be formed by the SOMO overlapping, which gives rise to kinetic exchange interactions. This is seen in molecular structures such as Kekulé structures (*e.g.*, Chichibabin's hydrocarbon)[7] or certain disjoint non-Kekulé structures (*e.g.*, tetramethylenethane).[8] The radical character of singlet diradicals varies with the magnitude of intramolecular exchange coupling,[9] and those with a small singlet–triplet energy gap are considered promising for next-generation materials, such as singlet fission.[10]

Nitroxides are a commonly used radical group due to their thermodynamic stability (>N–O• ↔ >N⁺•–O⁻) and help to reveal correlations between substituent positions and intramolecular exchange couplings in diradicals. For example, it has been reported that placing nitroxides at the 1,3-positions of a benzene ring (Scheme 1a) results in a triplet ground state,[11] while placing them at the 1,4-positions (Scheme 1b) results in a singlet ground state.[12] In addition, some bridging structures connecting two *tert*-butyl phenyl nitroxide moieties have been reported, such as vinylidene,[13] silole[14] and others.[15,16]

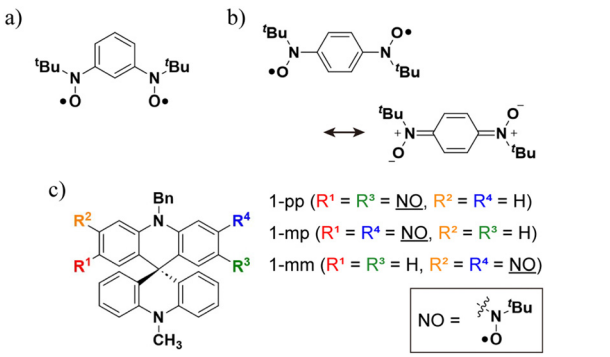

Scheme 1 (a) *m*-Phenylene[11a] and (b) *p*-phenylene bisnitroxide.[12a] (c) Diradicals **1-pp**, **1-mp** and **1-mm**.

In this study, we have focused on the exchange couplings through a sp^3-N atom with a lone pair. While such couplings have been previously reported in triradicals,[16] the relationship between the substituent positions of nitroxide diradicals and these interactions remains unclear. To reveal this relationship, we synthesized three novel diradicals with nitroxide groups at the 2,7-, 2,6- and 3,6-positions of 9,9′(10*H*,10′*H*)spirobiacridine (**1-pp**, **1-mp** and **1-mm**, respectively), as shown in Scheme 1c. In these compounds, the sp^3 carbon at the 9-position connects the two benzene rings, resulting in high coplanarity between them and limiting structural flexibility. In addition, the NH site is modified with a benzyl (Bn) group and its hyperconjugation with the methylene group of it suppresses the dynamics of the

Tokyo University of Science, 1-3 Kagurazaka, Shinjuku-ku, Tokyo, 162-8601, Japan. E-mail: kanetomo@rs.tus.ac.jp

† Electronic supplementary information (ESI) available: CCDC 2394806–2394808. For ESI and crystallographic data in CIF or other electronic format see DOI: https://doi.org/10.1039/d4cp04393f

NH site. These features allow a straightforward evaluation of the correlation between the different substitution positions of the nitroxide sites and their magnetic interactions. In fact, **1-pp** and **1-mm** exhibited the singlet ground state, whereas **1-mp** exhibited the triplet ground state. This radical-site dependence of the ground state in bisnitroxides is attributed to spin polarization. To the best of our knowledge, this finding is the first study on the exchange coupling through the lone pair of the sp^3-N atom in bisnitroxides.

Results and discussion

Synthesis and characterization

Compounds **1-pp**, **1-mp** and **1-mm** were synthesized according to the procedure shown in Scheme 2. For **1-mp** and **1-mm**, tetrabromodiphenylamine (**2**) was prepared *via* Buchwald–Hartwig cross-coupling between 2,4-/2,5-dibromoaniline and 1,4-dibromo-2-iodobenzen. The NH site of **2** was protected with the Bn group to give **3**. Subsequent lithiation of **3** with *n*-butyllithium followed by addition of *N*-methyl-9(10*H*)acridone afforded the spiro compounds (**4**). In addition, lithiation of **4** with *tert*-butyllithium followed by addition of 2-methyl-2-nitrosopropane afforded bishydroxylamine compounds (**5**). The synthesis of **5-pp** has been reported previously.[17] Diradicals **1** were obtained by oxidation of the bishydroxylamine derivatives with Ag_2O. Polycrystal samples of these diradicals were obtained by recrystallization from CH_2Cl_2 and *n*-hexane and characterized by spectroscopic and X-ray crystallographic analyses. Structural studies confirmed the presence of crystalline solvents (CH_2Cl_2) in all compounds, which easily escape under ambient conditions. In addition, **1-pp** may contain an impurity (3%), in which a *tert*-butyl nitroxide site is replaced by a Br group. This impurity is probably a by-product of the conversion of **4-pp** to **5-pp**. Elemental analysis was performed for **1-pp**, but accurate determination of the amount of impurity was difficult due to the minimal difference between the calculated values with and without the impurity (for details, see the ESI†). It is noted that the structural analysis successfully resolved the disorder components, and the low level of impurity in the bulk sample suggests that it does not significantly affect the interpretation of magnetic studies.

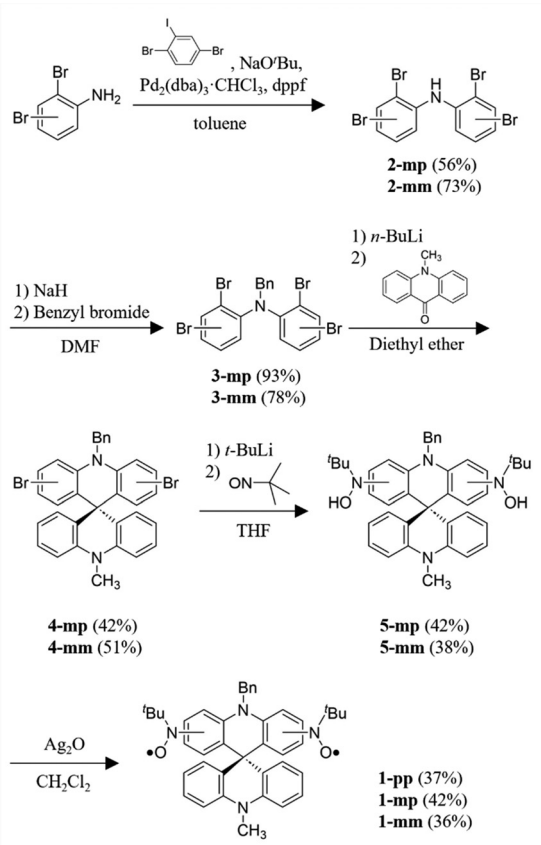

Scheme 2 Synthetic routes for **1-pp**, **1-mp** and **1-mm**.

Electron spin resonance (ESR) spectroscopy

The ESR spectra of **1-pp**, **1-mp** and **1-mm** recorded in toluene at room temperature are shown in Fig. S1–S3 (ESI†), respectively. All results exhibited a typical five-line spectrum, indicating that the exchange coupling constant (J) is larger than a hyperfine interaction (HFI).[1a,18] The g and a_N values for **1-pp**, **1-mp** and **1-mm** were estimated from simulation with *EasySpin* software,[19] giving 2.0076 and 0.5676 mT, 2.0074 and 0.5877 mT and 2.0077 and 0.5773 mT, respectively. In diradicals, the HFI constants with $J \gg$ HFI are half of those in the corresponding monoradicals. Based on the a_N values of **1-pp**, **1-mp** and **1-mm**, this gives HFI values of 1.12–1.16 mT for ^{14}N in the monoradical, which are relatively small among typical nitroxide species (1.0–1.5 mT).[20] A possible explanation is the delocalisation of the unpaired electron throughout the diphenylamine moiety due to spin extension from the nitroxide moieties to the phenyl groups. In fact, similar diradicals reported by Ohshita *et al.* exhibit small a_N values (0.580–0.660 mT).[15]

The frozen-solution ESR spectrum of **1-mp** in toluene at 77 K is shown in Fig. S4 (ESI†). The spectrum exhibited a zero-field splitting structure, indicating the triplet state. In addition, there was also a monoradical impurity. From the simulation, the $|D|/hc$ and $|E|/hc$ values are 4.00×10^{-3} cm^{-1} and 0.50×10^{-3} cm^{-1} with a g of 2.0080, and the ratio of the monoradical impurity was 15%. The point dipole approximation, $2D = 3g^2\mu_B/r^3$, with the experimental $|D|$, gave a dipole–dipole distance of 8.7 Å. This value is shorter than a crystallographically determined distance of 10.131(2) Å (for details, see below). This finding suggests that the radical spins are delocalized on these phenyl rings.

Crystal structures

Compound **1-pp** crystallized in the triclinic $P\bar{1}$ space group (Table S1, ESI†). The crystal structure is shown in Fig. 1a. There are disordered CH_2Cl_2 crystal solvents, which are accounted for in the SQUEEZE/PLATON program, and the electron count is 42 electrons per formula unit. This value is close to the one CH_2Cl_2 solvent (40 electrons). The N1–O1 and N2–O2 bond lengths are 1.279(3) and 1.289(2) Å, respectively. These bond lengths are close to the typical values of the nitroxide compounds (1.29 Å).[17] Torsion angles between the nitroxide and phenyl

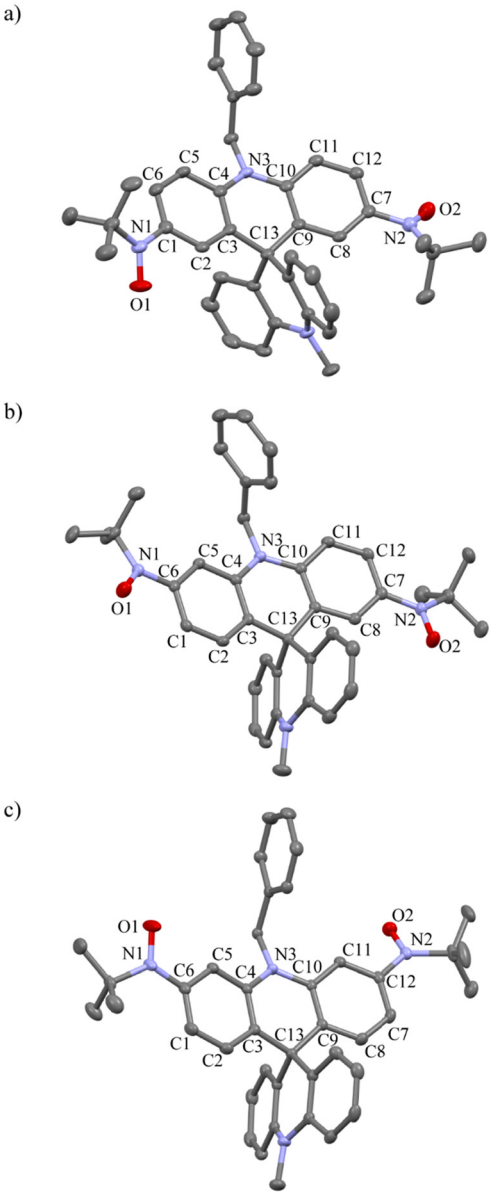

Fig. 1 Crystal structures of (a) **1-pp**, (b) **1-mp** and (c) **1-mm**. Thermal ellipsoids for non-hydrogen atoms are drawn at the 50% probability level. The H atoms are omitted for clarity. (a) The Br atom in **1-pp**, which is minor component, is also omitted for clarity.

moieties are −26.0(3)° for O1–N1–C1–C2 and −30.3(3)° for O2–N2–C7–C12. In addition, to confirm the coplanarity of two phenyl rings with nitroxides, the torsion angles C4–C3–C13–C9 and C10–C9–C13–C3 are 22.7(2)° and −22.0(2)°, respectively ($|\phi_{mean}|$ = 22.4°). The nearest intermolecular NO···NO distance is 4.210(2) Å of O2···O2, which is larger than the sum of the van der Waals (vdW) radii of O/O of 3.04 Å,[21] indicating no direct magnetic contacts.

Compound **1-mp** crystallized in the monoclinic $P2_1/c$ space group (Table S1, ESI†). The crystal structure is shown in Fig. 1b. There are disordered CH_2Cl_2 crystal solvents, which are accounted for in the SQUEEZE/PLATON program, and the electron count is 42 electrons per formula unit. This value is close to the one CH_2Cl_2 solvent (40 electrons). The N1–O1 and N2–O2 bond lengths are 1.282(2) and 1.288(2) Å, respectively. These bond lengths are close to the typical values of the nitroxide compounds (1.29 Å).[17] Torsion angles between the nitroxide and phenyl moieties are 13.5(2)° for O1–N1–C6–C1 and −18.8(2)° for O2–N2–C7–C8. In addition, to confirm the coplanarity of two phenyl rings with nitroxides, the torsion angles C4–C3–C13–C9 and C10–C9–C13–C3 are 14.2(2)° and −14.7(2)°, respectively ($|\phi_{mean}|$ = 14.5°). The nearest intermolecular NO···NO distance is 5.698(2) Å of O1···N3, which is larger than the sum of the vdW radii of O/N of 3.07 Å,[21] indicating no direct magnetic contacts.

Compound **1-mm** crystallized in the monoclinic $P2_1/c$ space group (Table S1, ESI†). The crystal structure is shown in Fig. 1c. There are disordered CH_2Cl_2 crystal solvents, which are accounted for in the SQUEEZE/PLATON program, and the electron count is 21 electrons per formula unit. This value is close to half of the CH_2Cl_2 solvent (20 electrons). The N1–O1 and N2–O2 bond lengths are 1.279(1) and 1.283(2) Å, respectively. These bond lengths are close to the typical values of the nitroxide compounds (1.29 Å).[17] Torsion angles between the nitroxide and phenyl moieties are −12.8(2)° for O1–N1–C6–C5 and −28.1(2)° for O2–N2–C12–C11. In addition, to confirm the coplanarity of two phenyl rings with nitroxides, the torsion angles C4–C3–C13–C9 and C10–C9–C13–C3 are 14.6(2)° and −19.2(2)°, respectively ($|\phi_{mean}|$ = 16.9°). The nearest intermolecular NO···NO distance is 4.198(2) Å of O2···O2, which is larger than the sum of the vdW radii of O/N of 3.04 Å,[21] indicating no direct magnetic contacts.

Theoretical calculations

Density functional theory (DFT) calculations were performed for **1-pp**, **1-mp** and **1-mm** during atomic coordination analysis based on the above crystallographic study. The calculated spin densities of the triplet (T) and broken-symmetry singlet (BS) states were mapped onto the molecular skeleton as shown in Fig. S5–S7 (ESI†). The triplet and singlet energy states are summarized in Table S2 (ESI†). Exchange coupling constants $2J/k_B$ for **1-pp**, **1-mp** and **1-mm** were −176.05, +56.89 and −11.45 K, respectively. Compounds **1-pp** and **1-mm** exhibit the singlet ground state, while **1-mp** exhibits the triplet ground state.

The intramolecular exchange coupling of diradicals **1** shows the dependence of the substituent positions according to the results of theoretical studies. These findings can be understood based on the combination of the periodicity of the π spins for phenyl nitroxide moieties and the lone pair on the bridging sp^3-N atom. Scheme 3a–c show the spin polarized maps for **1-pp**, **1-mm** and **1-mp**, respectively. In **1-pp**, the induced spins on the carbon adjacent to the sp^3-N atom, by spin polarization, are parallel to that on the *p*-positioned nitroxides. When spin polarization is also applied to the lone pair (two electrons) on the sp^3-N atom, the spins on the terminal nitroxides become an antiparallel configuration (singlet, S = 0; Scheme 3a). In addition, in **1-mm**, although the induced spins on these C atoms are antiparallel to that on the *m*-positioned nitroxides, the spins on the terminal nitroxides show the antiparallel configuration

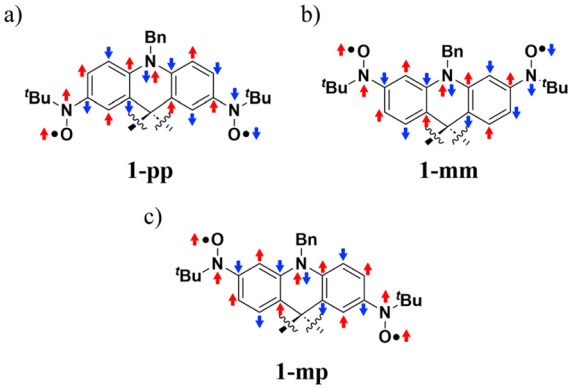

Scheme 3 Spin arrangements for (a) **1-pp**, (b) **1-mm** and (c) **1-mp** based on the spin polarization mechanism. Arrows on the structural formula denote that mechanism.

(singlet state, S = 0; Scheme 3b) owing to the pathway on the lone pair of the sp^3-N atom. On the other hand, in **1-mp**, the induced spins on the carbon adjacent to the sp^3-N atom are parallel and antiparallel to spins on the *p*- and *m*-positioned nitroxides, respectively. Through the lone pair of the sp^3-N atom, the terminal nitroxides exhibit the parallel configuration (triplet state, S = 1; Scheme 3c).

Both **1-pp** and **1-mm** exhibit the singlet ground state due to spin polarization, but the magnitude of interactions is significantly different (−176.05 K for **1-pp** *vs.* −11.45 K for **1-mm**). This difference is due to the structural nature of each compound, whether they adopt Kekulé or non-Kekulé structures. As shown in Scheme 3, spin polarization induces a polarized spin on the sp^3-N atom. Compounds **1-pp** and **1-mm** can be considered as 1,4- or 1,3-phenylene diradical motifs, respectively. The Kekulé structure of **1-pp** promotes a higher spin density on the sp^3-N atom, as shown in Scheme 1b. On the other hand, the non-Kekulé structure of **1-mm** results in a comparatively lower or negligible spin density. In fact, the spin density (ρ) on the sp^3-N atom in **1-pp** ($|\rho|$ = 0.0049) is larger than that in **1-mm** ($|\rho|$ = 0.0009). The other spin densities are listed in Table S3 (ESI†). This higher spin density in **1-pp** allows for a more effective exchange path, resulting in a lager exchange coupling constant than that of **1-mm**.

Finally, intermolecular interactions were also evaluated. Calculations for **1-pp**, **1-mp** and **1-mm** were performed based on the nearest intermolecular contacts described in the structure studies. The resulting exchange interactions were determined to be −1.44, −1.87 and −0.36, respectively (Table S4 and Fig. S8–S10, ESI†). All these interactions exhibited antiferromagnetic coupling. Moreover, the magnitude of these interactions suggested that intramolecular interactions dominate the magnetic properties of all compounds.

Magnetic properties

The magnetic susceptibilities were measured for polycrystalline **1-pp**, **1-pm** and **1-mm** at 2–300 K using a SQUID magnetometer (Fig. 2). It should be noted that the χ_mT value was calculated based on the formula weight without the crystalline solvents, as

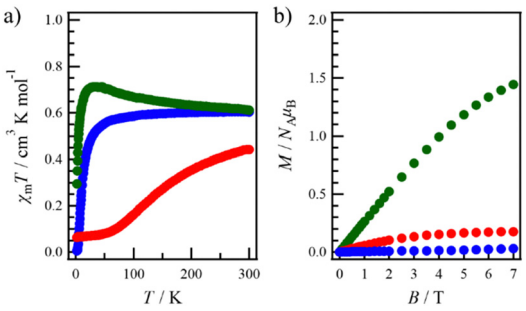

Fig. 2 (a) Temperature dependence of the product χ_mT measured at 5 kOe. (b) Field dependence of magnetization M measured at 2.0 K. Red, green and blue colours represent **1-pp**, **1-mp** and **1-mm**, respectively.

these evaporate easily. Quantitative assessments were addressed in the subsequent analysis of the magnetic measurements. In addition, for **1-pp**, the monoradical impurities were not included in the calculation of the χ_mT value, but it was evaluated in the later analysis.

First, the χ_mT *vs.* T plot for **1-pp** is shown in Fig. 2a. The χ_mT value at 300 K was 0.442 cm^3 K mol^{-1}, which is smaller than the value of 0.750 cm^3 K mol^{-1} expected for a species having two magnetically isolated radical spins (S = 1/2 and g = 2). This finding suggests the antiferromagnetic coupling and/or the presence of crystalline solvents. Upon cooling, χ_mT was gradually decreased and exhibited a plateau behaviour below 50 K, resulting in a χ_mT value of 0.0635 cm^3 K mol^{-1} at 2 K. The observed magnetic behaviour suggests intramolecular antiferromagnetic coupling, which is supported by DFT calculations. If **1-pp** has the singlet ground state, the χ_mT value would be zero. However, the χ_mT value observed in the plateau behaviour in the low-temperature region was not zero, indicating the presence of monoradical impurities. Here, the experimental data were analysed with the Bleaney–Bowers equation, eqn (1), based on the spin Hamiltonian, $H = -2JS_A \cdot S_B$.[22]

$$\chi_m T = \left(\frac{g^2 \mu_B{}^2 N_A}{k_B} \frac{1}{3 + \exp(-2J/k_B T)} f + \frac{g^2 \mu_B{}^2 N_A}{4k_B} (1 - f) \right) \times A \quad (1)$$

where J is the exchange coupling constant, g is fixed as 2.0076 as observed in the ESR study, f is a purity factor, and A is used for estimating the amount of crystalline solvents. To avoid overparameterization, intermolecular interaction was not considered in this analysis. The best fit curve gave $2J/k_B$ = −150.2(5) K, f = 0.7914(9) and A = 0.890(2), as shown in Fig. S8 (ESI†). The estimated $2J$ value was reproduced from the theoretical value (−176.05 K) derived from the DFT calculations. The purity factor f showed a larger proportion than expected from elemental analysis and structural analysis. This may be due to the presence of partially oxidized monoradical impurities from **5** in the bulk sample, which were not detected in our measurement. However, the presence of these impurities does not affect the evaluation of the exchange coupling of the diradicals, which is the focus of this study. From the A value, we estimated the amount of crystalline solvents CH_2Cl_2 (fw 84.93) to be 0.81 relative to **1-pp** (fw 622.78).

The field dependence of the magnetization (M) curve at 2 K is shown in Fig. 2b. The M value was saturated and reached 0.176 μ_B at 7 T. This value is assumed to be due to monoradical impurities, since the diradical shows zero. The calculation from the above purity factor f gives a value of 0.21 μ_B, which is close to the experimental result.

Next, the $\chi_m T$ *vs.* T plot for **1-mp** is shown in Fig. 2a. The $\chi_m T$ value at 300 K is 0.611 cm^3 K mol^{-1}, which is smaller than the expected value (0.750 cm^3 K mol^{-1}). This finding suggests the presence of crystalline solvents. Upon cooling, $\chi_m T$ was gradually increased and reached a peak at about 34 K (0.713 cm^3 K mol^{-1}). Upon further cooling, it decreased, reaching 0.295 cm^3 K mol^{-1} at 2 K. The increasing behaviour indicates the intramolecular ferromagnetic coupling, while the decreasing behaviour indicates the intermolecular antiferromagnetic coupling. The experimental data were analysed using eqn (2), which includes the Weiss constant (θ) and excludes the purity factor f in eqn (1).

$$\chi_m T = \left(\frac{g^2 \mu_B{}^2 N_A}{k_B} \frac{1}{3 + \exp(-2J/k_B T)} \frac{T}{T - \theta} \right) \times A \qquad (2)$$

The best fit curve gave $2J/k_B$ = +39(2) K, θ = −2.81(5) K and A = 0.788(3) with g = 2.0074 (fixed), as shown in Fig. S9 (ESI†). The estimated $2J$ and θ values were reproduced from the theoretical value (+56.89 K and −1.87 K) derived from the DFT calculations. From the A value, we estimated the amount of crystalline solvents CH_2Cl_2 (fw 84.93) to be 1.6 relative to **1-mp** (fw 622.78). The field dependence of the M curve at 2 K is shown in Fig. 2b. The M value at 7 T is not saturated (1.44 μ_B), which is smaller than expected for S = 1 (2 μ_B). From the A value, the experimental value becomes 1.83 μ_B, and considering no saturation, this result supports **1-mp** as the triplet ground state.

Finally, the $\chi_m T$ *vs.* T plot for **1-mm** is shown in Fig. 2a. The $\chi_m T$ value at 300 K is 0.602 cm^3 K mol^{-1}, which is smaller than the expected value (0.750 cm^3 K mol^{-1}). This finding suggests the presence of crystalline solvents. Upon cooling, $\chi_m T$ showed an abrupt decreasing behaviour around 30 K, and the $\chi_m T$ value at 2 K was 0.00443 cm^3 K mol^{-1}. This behaviour indicates the intramolecular antiferromagnetic coupling. The experimental data was analysed using eqn (2). The best fit curve gave $2J/k_B$ = −9.08(4) K, θ = −0.38(5) K and A = 0.8168(4) with g = 2.077 (fixed). The estimated $2J$ and θ values are reproduced from the theoretical value (−11.45 K and −0.36 K) derived from the DFT calculations. From the A value, we estimated the amount of crystalline solvents CH_2Cl_2 (fw 84.93) to be 1.4 relative to **1-mm** (fw 622.78). The field dependence of the M curve at 2 K is shown in Fig. 2b (blue markers). The M value exhibits almost zero (0.0310 μ_B at 7 T). This finding supports **1-mm** as the singlet ground state (S = 0).

Conclusions

In this study, three novel acridane-based bisnitroxides (**1-pp**, **1-mp** and **1-mm**) were synthesized, each differing in the positions of their radical groups. Theoretical studies revealed that **1-pp** and **1-mm** exhibit the singlet ground state (S = 0), while **1-mp** exhibits the triplet ground state (S = 1). In addition, the difference in the interaction magnitude between **1-pp** and **1-mm** was observed, indicating variations in the effective delocalization of the radical spins *via* the π-conjugated system and lone pair on the sp^3-N atom, depending on the radical positions. These theoretical results are supported by experimental magnetic studies. This study shows that, despite sharing the same π-conjugated framework, the position of the radical groups leads to substantial differences in the singlet–triplet energy gaps. To control this energy gap, these results suggest that it is important not only to extend the π-conjugated system (a typical approach), but also to carefully select the substituent positions of the radical centres.

Data availability

The data supporting this article have been included as part of the ESI.† Crystallographic data for **1-pp**, **1-mp** and **1-mm** have been deposited at the CCDC numbers under 2394806–2394808.

Conflicts of interest

There are no conflicts to declare.

Acknowledgements

This study was financially supported by the KAKENHI (JSPS, 20K22538 and 24K17661). The crystallography works for **1-pp**, **1-mp** and **1-mm** were conducted at the Advanced Characterization Nanotechnology Platform of the University of Tokyo, supported by the "Nanotechnology Platform" of the MEXT, Japan.

Notes and references

1 (*a*) M. Abe, Diradicals, *Chem. Rev.*, 2013, **113**, 7011–7088; (*b*) N. M. Gallagher, A. Olankitwanit and A. Rajca, High-Spin Organic Molecules, *J. Org. Chem.*, 2015, **80**, 1291–1298; (*c*) C. Shu, Z. Yang and A. Rajca, From Stable Radicals to Thermally Robust High-Spin Diradicals and Triradicals, *Chem. Rev.*, 2023, **123**, 11954–12003.

2 W. T. Borden, R. Hoffmann, T. Stuyver and B. Chen, Dioxygen: What Makes This Triplet Diradical Kinetically Persistent?, *J. Am. Chem. Soc.*, 2017, **139**, 9010–9018.

3 (*a*) A. Ito, M. Urabe and K. Tanaka, A Spiro-Fused Triarylaminium Radical Cation with a Triplet Ground State, *Angew. Chem., Int. Ed.*, 2003, **42**, 921–924; (*b*) T. Kanetomo, K. Ichihashi, M. Enomoto and T. Ishida, Ground Triplet Spirobiradical: 2,2′,7,7′-Tetra(*tert*-butyl)-9,9′(10*H*,10′*H*)-spirobiacridine-10,10′-dioxyl, *Org. Lett.*, 2019, **21**, 3909–3912; (*c*) S. Ogawa, T. Kanetomo and M. Enomoto, Spiro-centre substitution effects in the intramolecular spin–spin interactions of spirobiacridine diradicals, *Org. Chem. Front.*, 2024, **11**, 3004–3011.

4 P. Dowd, Trimethylenemethane, *Acc. Chem. Res.*, 1972, **5**, 242–248.

5 (*a*) H. Nishimaki and T. Ishida, Organic Two-Step Spin-Transition-Like Behavior in a Linear S = 1 Array: 3′-Methylbiphenyl-3,5-diyl Bis(*tert*-butylnitroxide) and Related Compounds, *J. Am. Chem. Soc.*, 2010, **132**, 9598–9599; (*b*) H. Phan, T. S. Herng, D. Wang, X. Li, W. Zeng, J. Ding, K. P. Loh, A. T. S. Wee and J. Wu, Room-Temperature Magnets Based on 1,3,5-Triazine-Linked Porous Organic Radical Frameworks, *Chem*, 2019, **5**, 1223–1234; (*c*) H. Hamamoto, D. Shimizu and K. Matsuda, Verdazyl–Nitroxide Diradical with S = 1 Ground State: Observation of Long-Range Ordering and Haldane Gap in a Highly Isotropic S = 1 Antiferromagnetic Heisenberg Chain, *J. Phys. Chem. C*, 2023, **127**, 21822–21828; (*d*) T. Kanetomo, D. Matsunaga, S. Ogawa and M. Enomoto, Anomalous magnetic behaviour induced by a structural phase transition with anisotropic thermal expansion in a spirodiradical, *Org. Chem. Front.*, 2024, **11**, 6495–6502.

6 (*a*) H. Iwamura, K. Inoue and N. Koga, Tacticity versus dimension of the extended structures in the crystals of heterospin magnets made of transition-metal complexes with the poly(aminoxyl) radical, *New J. Chem.*, 1998, **22**, 201–210; (*b*) E. M. Fatila, R. Clérac, M. Rouières, D. V. Soldatov, M. Jennings and K. E. Preuss, High-Spin Ribbons and Antiferromagnetic Ordering of a Mn^{II}-Biradical-Mn^{II} Complex, *J. Am. Chem. Soc.*, 2013, **135**, 13298–13301; (*c*) T. Kanetomo, Y. Naoi and M. Enomoto, Gadolinium-Triradical Complex with Ground S = 10 State: Synthesis, Structural Characterization and Magnetic Studies, *Eur. J. Inorg. Chem.*, 2021, 1130–1136; (*d*) S. Ito, R. Takano, S. Hatanaka and T. Ishida, Rare-Earth (RE = Y, Gd, Tb, Dy, Ho, and Er) Chains Bridged with a Triplet Biradical and Magnetic Hysteresis Recorded for RE = Tb, *Inorg. Chem.*, 2022, **61**, 10619–10623.

7 A. E. Tschitschibabin, Über einige phenylierte Derivate des *p*,*p*-Ditolyls, *Chem. Ber.*, 1907, **40**, 1810–1819.

8 C. J. Cramer, Paul Dowd and diradicals, *J. Chem. Soc., Perkin Trans. 2*, 1998, 1007–1014.

9 T. Kubo, Recent Progress in Quinoidal Singlet Biradical Molecules, *Chem. Lett.*, 2015, **44**, 111–122.

10 T. Minami and M. Nakano, Diradical Character View of Singlet Fission, *J. Phys. Chem. Lett.*, 2012, **3**, 145–150.

11 (*a*) K. Mukai, H. Nagai and K. Ishizu, The Proof of a Triplet Ground State in the *N*,*N*′-Di-*t*-butyl-*m*-phenylenebinitroxide Biradical, *Bull. Chem. Soc. Jpn.*, 1975, **48**, 2381–2382; (*b*) G. Spagnol, K. Shiraishi, S. Rajca and A. Rajca, Triplet ground state (S = 1) pegylated bis(aminoxyl) diradical: synthesis and the effect of water on magnetic properties, *Chem. Commun.*, 2005, 5047–5049; (*c*) H. Nishimaki, S. Mashiyama, M. Yasui, T. Nogami and T. Ishida, Bistable Polymorphs Showing Diamagnetic and Paramagnetic States of an Organic Crystalline Biradical Biphenyl-3,5-diyl Bis(*tert*-butylnitroxide), *Chem. Mater.*, 2006, **18**, 3602–3604; (*d*) T. Yoshitake, H. Kudo and T. Ishida, Thermally Activated Paramagnets from Diamagnetic Polymers of Biphenyl-3,5-diyl bis(*tert*-butyl Nitroxides) Carrying Methyl and Fluoro Groups at the 2′- and 5′-Positions, *Crystals*, 2016, **6**, 30.

12 (*a*) S. Nakazono, S. Karasawa, N. Koga and H. Iwamura, Stabilization of *p*-Phenylenebis(*N*-*tert*-butylaminoxyl) Relative to *p*-Benzoquinonediimine *N*,*N*′-Dioxide, *Angew. Chem., Int. Ed.*, 1998, **37**, 1550–1552; (*b*) P. Ravat and M. Baumgarten, ''Tschitschibabin type biradicals'': benzenoid or quinoid?, *Phys. Chem. Chem. Phys.*, 2015, **17**, 983–991.

13 (*a*) T. Matsumoto, T. Ishida, N. Koga and H. Iwamura, Intramolecular Magnetic Coupling between Two Nitrene or Two Nitroxide Units through 1,1-Diphenylethylene Chromophores. Isomeric Dinitrenes and Dinitroxides Related in Connectivity to Trimethylenemethane, Tetramethyleneethane, and Pentamethylenepropane, *J. Am. Chem. Soc.*, 1992, **114**, 9952–9959; (*b*) D. A. Shultz, R. M. Fico Jr., H. Lee, J. W. Kampf, K. Kirschbaum, A. A. Pinkerton and P. D. Boyle, Mechanisms of Exchange Modulation in Trimethylenemethane-type Biradicals: The Roles of Conformation and Spin Density, *J. Am. Chem. Soc.*, 2003, **125**, 15426–15432.

14 N. Roques, P. Gerbier, U. Schatzschneider, J.-P. Sutter, P. Guionneau, J. Vidal-Gancedo, J. Veciana, E. Rentschler and C. Guérin, Experimental and Theoretical Studies of Magnetic Exchange in Silole-Bridged Diradicals, *Chem. – Eur. J.*, 2006, **12**, 5547–5562.

15 J. Ohshita, T. Iida, N. Ohta, K. Komaguchi, M. Shiotani and A. Kunai, Synthesis of Phenylnitroxides Bridged by an sp^3-Linkage, *Org. Lett.*, 2002, **4**, 403–406.

16 (*a*) T. Itoh, K. Matsuda, H. Iwamura and K. Hori, Tris[*p*-(*N*-oxyl-*N*-*tert*-butylamino)phenyl]amine, -methyl, and -borane Have Doublet, Triplet, and Doublet Ground States, Respectively, *J. Am. Chem. Soc.*, 2000, **122**, 2567–2576; (*b*) S. Suzuki, A. Nagata, M. Kuratsu, M. Kozaki, R. Tanaka, D. Shiomi, K. Sugisaki, K. Toyota, K. Sato, T. Takui and K. Okada, Trinitroxide-Trioxytriphenylamine: Spin-State Conversion from Triradical Doublet to Diradical Cation Triplet by Oxidative Modulation of a *p*-Conjugated System, *Angew. Chem., Int. Ed.*, 2012, **51**, 3193–3197.

17 T. Kanetomo, S. Ono, Y. Fukushima, Y. Takenouchi and M. Enomoto, Galvinoxyl-inspired dinitronyl nitroxide: structural, magnetic, and theoretical studies, *Org. Chem. Front.*, 2023, **10**, 3193–3200.

18 R. Uesugi, R. Takano and T. Ishida, Biradical pincers involving two phenylene, biphenylene or terphenylene arms: Evidence for approach of two terminal nitroxides, *Tetrahedron*, 2024, **156**, 133929.

19 S. Stoll and A. Schweiger, EasySpin, a comprehensive software package for spectral simulation and analysis in EPR, *J. Magn. Reson.*, 2006, **178**, 42–55.

20 A. K. Hoffmann, A. M. Feldman and E. Gelblum, Reactions of Organoalkali Compounds with Nitro Compounds: A New Synthesis of Nitroxides, *J. Am. Chem. Soc.*, 1964, **86**, 646–650.

21 A. Bondi, van der Waals Volumes and Radii, *J. Phys. Chem.*, 1964, **68**, 441–451.

22 B. Bleaney and K. D. Bowers, Anomalous paramagnetism of copper acetate, *Proc. R. Soc. London, Ser. A*, 1952, **214**, 451–465.